International Journal of Civil Engineering
https://doi.org/10.1007/s40999-023-00937-y

RESEARCH PAPER

# Mechanical properties and structural behaviors of reinforced concrete beams subjected to various degrees of corrosion

Thanh-Hung Nguyen[1] · Hoang-Thach Vuong[1] · Duy-Duan Nguyen[2] · Van Cong Chien[1] · Duy-Kien Dao[1]

Received: 14 February 2023 / Revised: 28 November 2023 / Accepted: 15 December 2023


## Abstract
This study aimed to evaluate the mechanical properties and structural behaviors of reinforced concrete (RC) beams with various corrosion levels. For this purpose, six RC beams were subjected to accelerated corrosion tests, with three pairs corresponding to 1-month, 2-month, and 3-month corrosion degrees. After corrosion tests, the corroded reinforcing bars and concrete were tested to measure the mechanical properties of the materials, such as reinforcement strength, concrete strength, reinforcement diameter reduction, and rebar weight loss. Additionally, the three corroded RC beams with three levels of corrosion were subjected to bending tests to determine their remaining structural capacity and failure patterns. Furthermore, Atena software was used to perform a series of numerical finite element methods to verify the experiment results, which indicated that a good agreement of structural behaviors was observed between the experiment and FEM analysis. FEM analysis is successful when the error of maximum force between experiment and simulation is less than 3% and the error of displacement at maximum load between simulation and experiment is less than 1.8%. The results showed that the load–defection relationships and crack patterns of corroded RC beams were significantly influenced by corrosion level. In addition, predicting the dangerous cross-section of steel structures will support maintenance work to reduce risks for the project.

**Keywords** Accelerated corrosion · RC beams · Bending capacity · Failure mode · Residual strength

## 1 Introduction

Every year, corrosion causes severe damage to the workings of reinforced concrete (RC) structures. Corrosion reduces the cross-sectional area of reinforcement working with concrete; thus, the bearing capacity and other behaviors of RC structures also decrease. In addition, corrosion pollutes the environment because corrosion products, such as iron oxides and coatings, are absorbed into the soil and water [1].

The reinforcement corrosion process in concrete can be divided into three main stages, each of which has its own characteristics. Stage 1 is the chloride penetration stage. Steel begins to react with passive reduction, leading to corrosion of the reinforcement in the areas where chloride penetrates; this chloride penetration process usually begins at the contiguous regions between steel and concrete or gaps in concrete [2–4]. In Stage 2, chloride covers and causes corrosion to the reinforcement; at this time, the adhesion of concrete and reinforcement begins to decline,

✉ Duy-Kien Dao
kiendd@hcmute.edu.vn

Thanh-Hung Nguyen
nthung@hcmute.edu.vn

Hoang-Thach Vuong
thachvh.ncs@hcmute.edu.vn

Duy-Duan Nguyen
duyduankxd@vinhuni.edu.vn

Van Cong Chien
1880813@student.hcmute.edu.vn

1 Department of Civil Engineering, University of Technology and Education Ho Chi Minh City, No 1 Vo Van Ngan Street, Linh Chieu Ward, Thu Duc City, Ho Chi Minh City, Vietnam

2 Department of Civil Engineering, Vinh University, Vinh 461010, Vietnam

Published online: 15 February 2024

and the openings develop, allowing chloride to penetrate deeper. More leads to faster corrosion propagation, and the steel surface starts to corrode, distributed and localized. When the reinforcement is corroded, the volume of the reinforcement increases, which leads to the concrete being cracked by steel; at this stage, small cracks will appear [5]. Stage 3 is a period of rapid corrosion development in which the locally corroded parts cause the steel section to decrease locally, along with the effect of the working load. It is possible to imagine that the reinforcement is both worn and fatigued. As a result, the structural capacity of RC structures is also reduced and can lead to failure [6–9].

When the reinforcements within the concrete are corroded, steel ribs are used to increase the adhesion force of the concrete. When the steel beam is subjected to bending, it is also gradually lost due to corrosion. This steel ribbed part is also a critical component in maintaining the flexural capacity of the beam when designing [10, 11]. Moreover, in addition to the reduced adhesion, the appearance of steel rust also causes the reinforcement and concrete to separate, which loses the ability to work simultaneously with steel and concrete. The bending treatment is further degraded [6, 12–14].

A high-quality bond between reinforcements and concrete plays an important role in increasing the transmission of tensile stress and enhancing flexural capacity. This effect in RC members is explained by the fact that the concrete in between the cracks carries tensile stress. Consequently, the active rebar is stiffer than the raw bar and shows the formation of multiple closely spaced cracks [15, 16]. A study of corroded beams, performed by [17, 18], showed that cross-sectional and bond reduction significantly affected the stiffness and flexural strength of the RC beam. This is achieved by creating local nicks on the reinforcement and removing the local coating, which demonstrates the role of stress transmission between the concrete and reinforcing bars and the notch locations. Regarding stiffness and flexural capacity, an increasing degree of corrosion failure has been shown to cause flexural cracks to widen and reduce their number, at least in relation to the inhomogeneity of reinforcement corrosion [8]. However, corrosion-induced bond deterioration reduces the stress transfer between rebars and concrete, and thereby, the effects of hardening are decreased [19]. This justifies the reduction of flexural cracks. Therefore, it is necessary to further investigate the impact of bond deterioration on the deflection and damaged patterns of corroded RC beams subjected to bending.

This study aims to evaluate the mechanical properties and structural behaviors of corroded RC beams by considering various corrosion levels. First, the RC beams were subjected to accelerated corrosion at different levels. Next, the corroded reinforcing bars and concrete were tested to measure the mechanical properties of the materials, such as reinforcement strength, concrete strength, reinforcement diameter reduction, and rebar weight loss. Additionally, the three corroded RC beams with three levels of corrosion were subjected to bending tests to determine the remaining structural capacity and failure patterns. Furthermore, a series of numerical simulations was performed to verify the results of the experiments.

## 2 Test programmes

### 2.1 Description of RC beam specimens

The tested RC beams contained two longitudinal reinforcements with a diameter of 16 mm in the tensile zone, two rebars with a diameter of 12 mm in the compressive zone, and stirrups with a diameter of 6 mm. The properties of the reinforcement are shown in Table 1. The width and height of the cross-sections of the beams were 200 mm and 300 mm, respectively, while the total length of all RC beams was 3.3 m, as shown in Fig. 1. In this study, six beams were grouped into three pairs to test three accelerated corrosion grades (one month, two months, and three months). The concrete composition is shown in Table 2.

After concrete casting, the beams are cured in 28 days in a chamber with maintaining the temperature of 25 °C and humidity of 90% during the curing process. Next, three pairs of the beams are imposed in the series of accelerated corrosion tests considering 10%, 25%, and 40% mass loss levels of reinforcing bars. These three types of beams are referred as C1, C2, and C3, respectively. It should be noted that each pair of corroded beams is fabricated from the same batch.

### 2.2 Accelerated corrosion tests

Three pairs of the beams are, therefore, imposed to the accelerated corrosion tests using the impressed current, as shown in Fig. 3a. To speed up the corrosion of the reinforcing bars, the RC beams are embedded in a salt 3.0% NaCl solution. At the same time, the reinforcements of

**Table 1** Mechanical properties of reinforcements

| Type | Yield strength, $f_y$ (MPa) | Ultimate strength, $f_u$ (MPa) | Elastic modulus, $E_s$ (GPa) | Area ($mm^2$) |
|---|---|---|---|---|
| Φ6 | 378.5 | 543 | 200 | 28.2 |
| Φ12 | 364.1 | 508.7 | 200 | 78.5 |
| Φ16 | 353.4 | 499.4 | 200 | 314.2 |

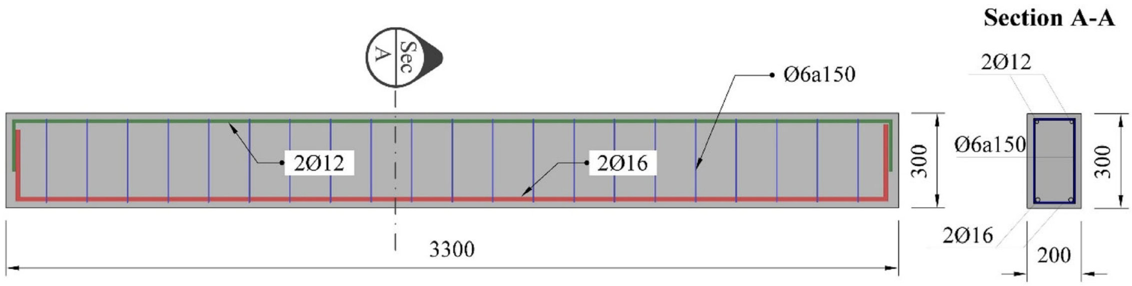


**Fig. 1** Configurations of RC beams

**Table 2** Proportions of concrete

| Water, W (lit) | Cement, C (kg) | W/C | Sand (kg) | Stone (kg) | Slump (cm) | Strength, $f'_c$ (MPa) |
|---|---|---|---|---|---|---|
| 188 | 328 | 0.573 | 594 | 1,123 | 6 | 26.3 |

three pairs of RC beams are continuously connected to a direct current of 900 μA/cm$^2$ in 1 month, 2 months, and 3 months, respectively. It should be noted that reinforcements are connected to the current anode, meanwhile the negative electrode of the current is connected to a copper rod.

The electric current is adjusted to maintain the intensity of 900 μA/cm$^2$ during the tests. This adjustment is calculated based on the area of the reinforcing bars. A relationship between the corrosion time and the percentage of weight loss of reinforcing bars is expressed by the following equation [20].

$$\begin{aligned} WL &= 0.235I \times t \quad (\text{if } I \times t < 66 \text{ A.hr}), \\ WL &= 0.617I \times t - 25.305 \quad (\text{if } I \times t > 66 \text{ A.hr}), \end{aligned} \tag{1}$$

where $WL$ denotes the reinforcement weight loss (g), $t$ represents the corrosion time (hr), $I$ = 3.618 A (i.e., the electric intensity). Table 3 shows the required time for corrosion tests of three pairs of beams.

All RC beams were moved to the immersion tank and the solution of electrolysis was set up so that the RC beams were corroded. The beam was completely immersed in 3% NaCl solution as shown in Fig. 2. It is important to note that the experiments are regularly monitored, checked and

**Table 3** Required time for accelerated corrosion tests

| RC beam | Weight loss of reinforcement | Weight loss of reinforcement, $W$ (g) | Time, $t$ (hr) |
|---|---|---|---|
| C1 | 7% | 1582 | 720 |
| C2 | 14% | 3189 | 1440 |
| C3 | 21% | 4796 | 2160 |

maintained to ensure a stable operation. After 07 days of testing, the surface of reinforcing bars appeared reddish rust in the position adjacent to the water level. After 30 days, the reinforcing bars were connected to the source also were rusted with scales from 0.5 mm to 1 mm, as shown in Fig. 3b. After finishing corrosion tests, one beam in each pair was chosen to crush the concrete and then extract reinforcements for weighting the longitudinal and transversal bars. Also, the tensile strength of corroded rebars was tested and the reinforcement mass loss due to corrosion was measured. Details in these measurements are presented in the following sections.

### 2.3 Mass loss measurement of rebars

After corrosion tests, the mass loss was determined by extracting the rebars from the beams. Using caliper to determine the least, the intermediate, and the most corroded segments, as shown in Fig. 4.

### 2.4 Strength of rebars and concrete after corrosion tests

In addition to measure the rebar mass loss, the corroded longitudinal reinforcing bars were also tested to observe its remaining strengths. The rebars were cut into segments with 600–800 mm long, as shown in Fig. 5. Additionally, the strength of concrete of the corroded RC beams was measured by drilling to take concrete specimens and then testing to obtain the compressive strength, as shown in Fig. 6.

### 2.5 Four-point bending tests of corroded RC beams

After accelerated corrosion tests, the corroded RC beams were imposed to four-point bending tests to obtain the load–deflection relationships and the failure patterns. The set-up of four-point bending tests is shown in Fig. 7. The span of applied loads was 1.6 m, and the distance from supports to the beam ends was 150 mm. In this study, a 500

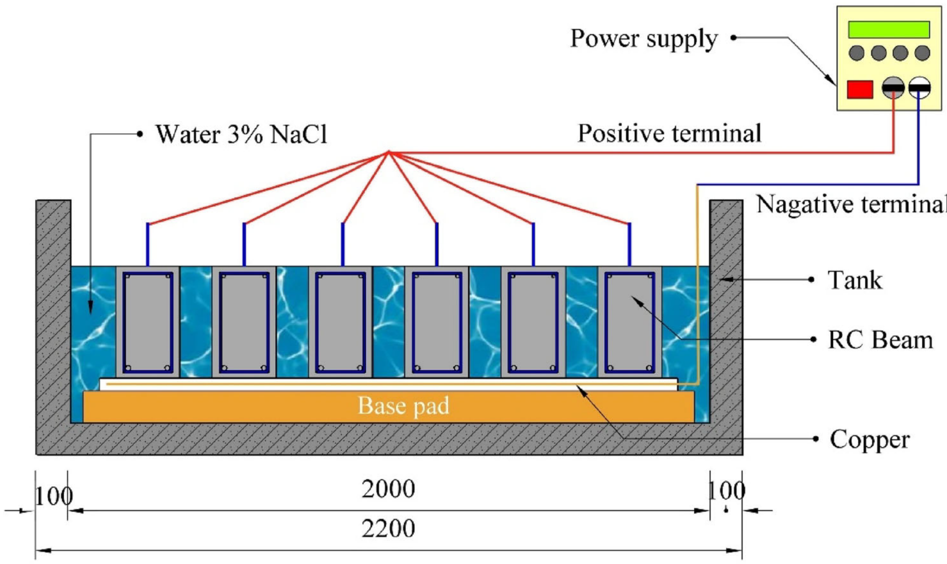


**Fig. 2** Accelerated corrosion setup


(a) Starting of corrosion test


(b) Corroded specimens

**Fig. 3** Accelerated corrosion tests of RC beams

kN load cell, which was applied at the mid-span of the beams. To reduce the local damage during the load transferring a rectangular steel plate with dimensions 70 × 150 mm was attached to the loading points. The pined supports were made by steel and have a diameter of 4 cm. It should be noted that the loading rate of 0.03 kN/s was applied during the tests to monitor the cumulative behavior of the beams. To measure the deflection of the corroded RC beams, two vertical linear variable differential transformers (LVDTs) were attached to the bottom mid-span of the beams, as shown in Fig. 7.

## 2.6 Experimental results and discussion

### 2.6.1 Weight loss of rebars due to corrosion

The weight loss of reinforcements was decided by extracting the rebars from the corroded beams after crushing concrete. A caliper was used to measure the corroded reinforcements. Additionally, the weight of corroded rebars were measured to quantify the loss due to corrosion effects. Table 4 shows the loss and remaining weights of the reinforcements in three corroded beams. It can be observed that after 1-month corrosion, the weight of reinforcements was reduced 11%. Meanwhile, it was lost 14% and 25% for the 2-month and 3-month RC beams induced corrosion, respectively.

### 2.6.2 Residual strength of concrete and steel due to corrosion

Figure 8 demonstrates the decrease of the compressive strength of concrete with various degrees of corrosion. The mean and standard deviation of each of beams are indicated that the strength of concrete in beam C1 reduced 22.4% compared with the non-corroded RC beam (C0). Whereas


**Fig. 4** Measuring the diameter of reinforcing bars after corrosion tests

**Fig. 5** Tensile tests for corroded reinforcing bars

the concrete strength of beams C2 and C3 reduced 31.2% and 33.6%, respectively, in comparison with that of beam C0. These experimental results confirm that the corrosion process has deteriorated the compressive strength of concrete significantly.

Moreover, the effects of corrosion on the longitudinal reinforcement are evaluated, as shown in Fig. 9. Four parameters, which were the rebar diameter reduction, mass loss per unit of length, total mass loss, and tensile strength reduction were quantified for three corroded beams. The sampling procedure of tensile rebars are obeyed. Figure 9a presents the reduction of the rebar diameter, mass loss per unit of length, total mass loss, and tensile strength with respect to three levels of corrosion at LVDT1 and LVDT3.


(a) Drilling to take concrete specimens


(b) Compresive tests

**Fig. 6** Compressive tests of concrete specimens

In particular, the tensile rebar diameter of beam C1 were reduced by 6.9%, 24.4%, and 38.5% at LVDT1, LVDT2, and LVDT3, respectively. While the reductions in cases of beam C2 and C3 at LVDT1, LVDT2, and LVDT3 were 15.63%, 40.8%, 46.3% and 22.5%, 44.7%, 52.5%, respectively. Figure 9b shows the mass loss in a unit length of beam C1, C2 at LVDT1, LVDT2, and LVDT3 were 12.2%, 42.3%, 61.3% and 28.2%, 64.8%, 70.5%, respectively. Whereas it was decreased by 39.1%, 69.3%, 80% for beam C3. Figure 9c summarizes the total mass loss of reinforcements in corroded beams C1, C2, and C3 in comparison with the uncorroded beam C0. It can be seen that the percentage of total mass reduction due to the corrosion of beam C1, C2, and C3 were 11.3%, 14.4%, and 24.8%, respectively. Finally, the residual tensile strengths of corroded tensile rebars are shown in Fig. 9d. The tensile strength of corroded rebar was significantly decreased from C0 to C3. The degraded magnitude was proportional to the corrosion time as well as the locations of the corroded beam. Specifically, the percentage of tensile strength reduction for C1 and C3 at LVDT1, LVDT2, LVDT3 were 1.3%, 15.7%, 35.6% and 11.5%, 39%, 72.6%, respectively.

The load–displacement curves of corroded longitudinal rebar in tensile tests are shown in Fig. Figure 10. For corroded reinforcements, it showed that the reduction of reinforcement tensile strength was very significant, and the law of the curve was not clear compared to that of the non-corroded reinforcement. Moreover, the ductility of the corroded reinforcement was pronouncedly reduced, as shown in Fig. 10a. The corroded reinforcement had a greater hardness than the uncorroded reinforcement when the corrosion level of 11%, as shown in Fig. 10b; however, the stiffness was reduced when the corrosion level up to 25%, as shown in Fig. 10c, d.

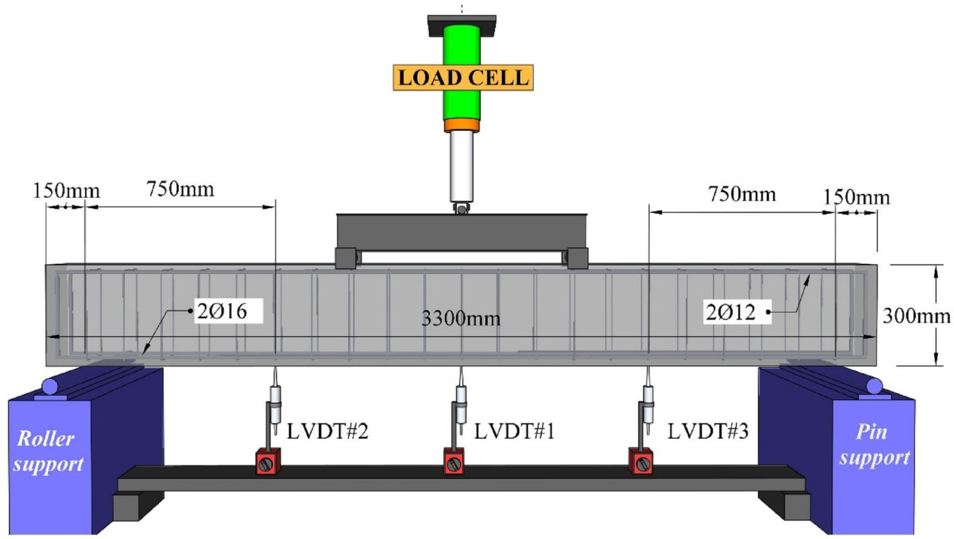


(a)

(b)

**Fig. 7** Loading setup: **a** schematic diagram and **b** test set-up

**Table 4** Summary of corrosion process in term of weight loss

| RC beam | Original mass (kg) | Remained mass (kg) | Weight loss of steel, *W* (g) | Weight loss of steel, % | Time, *t* (hr) |
|---|---|---|---|---|---|
| C1 | 23 | 20.40 | 2.60 | 11% | 720 |
| C2 | 23 | 19.70 | 3.30 | 14% | 1440 |
| C3 | 23 | 17.30 | 5.70 | 25% | 2160 |

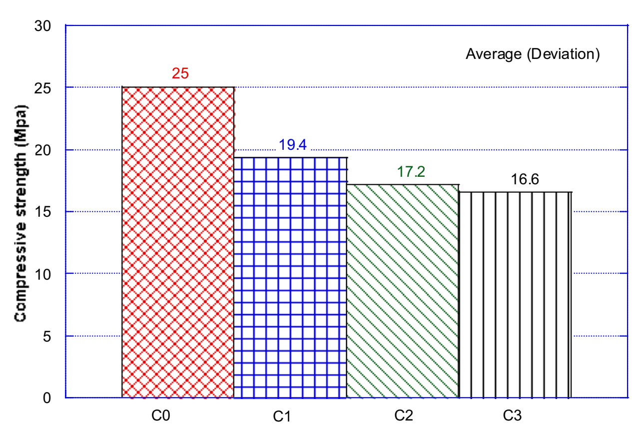


**Fig. 8** Compressive strength of concrete

### 2.6.3 Load–displacement relation of corroded RC beams

The load–deflection relationship of all tested beams is subjected to various levels of corrosion was inspected.

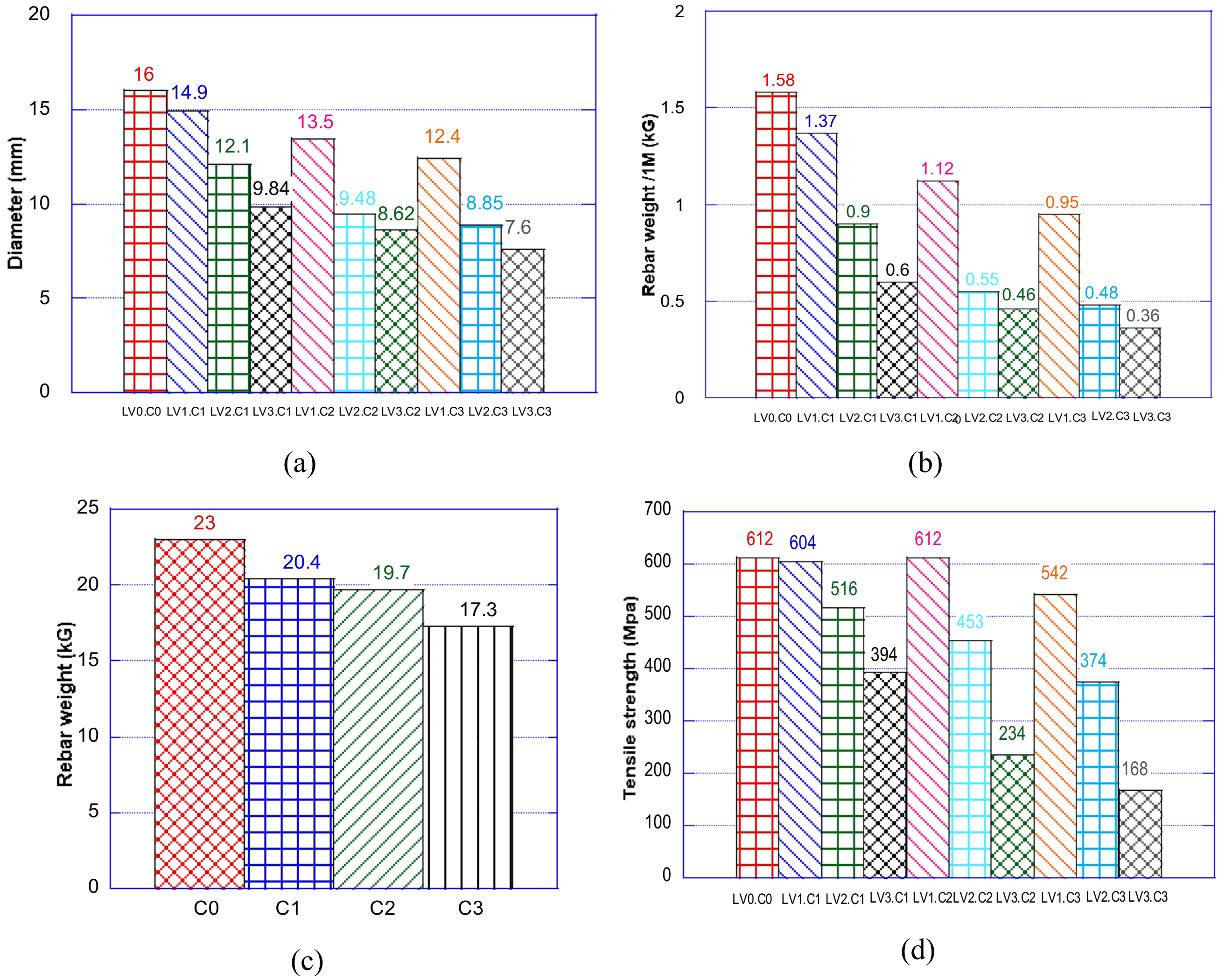


**Fig. 9** Effects of corrosion on the strength of longitudinal reinforcing bars

Figure 11 reveals the complexity of the load–deflection relationship of RC beams subjected to the different levels of corrosion. Indeed, in the elastic phase for the load range from 0 to 20 kN, the stiffness of all beams is similar to each other. From a load of 20 kN or more, the stiffness of the beams changes more clearly, especially for beam C2; although the level of reinforcement and concrete penetration is greater than that of beam C1, the stiffness of C2 beams is more significant than that of C1. Figure 11 shows that the stiffness of C2 is more significant than C1 and C0. This shows that with the corrosion level of the C2 beam, the connection between the reinforcement and concrete was better, and the reinforcement increased the hardness but turned to a more brittle state when the reinforcement was not corroded. The beam bending test results showed that the beam C1 had a 6.25% reduction in load capacity compared to the uncorroded beam C0, while the loading capacity of the beam C2 and C3 was reduced by 25% and 43.75%, respectively.

### 2.6.4 Crack patterns

Figure 12 shows that in accordance with the rule, the distribution is concentrated in the area between the beams with large displacement, the distance between the cracks is more considerable. The cracks are even from the bottom of the beam up to the top of the beam. The corroded beams C1, C2, C3 all appeared the first visible crack at the load level from 24 to 26 kN. The number of cracks were less than that of the C0 beam because the concrete was degraded by corrosion. The tensile strength of concrete was reduced. The number of cracks of the corroded beams were decreased from C1 to C3; and cracking were mainly from the bottom to half of the beam, 1 or 2 cracks appeared from

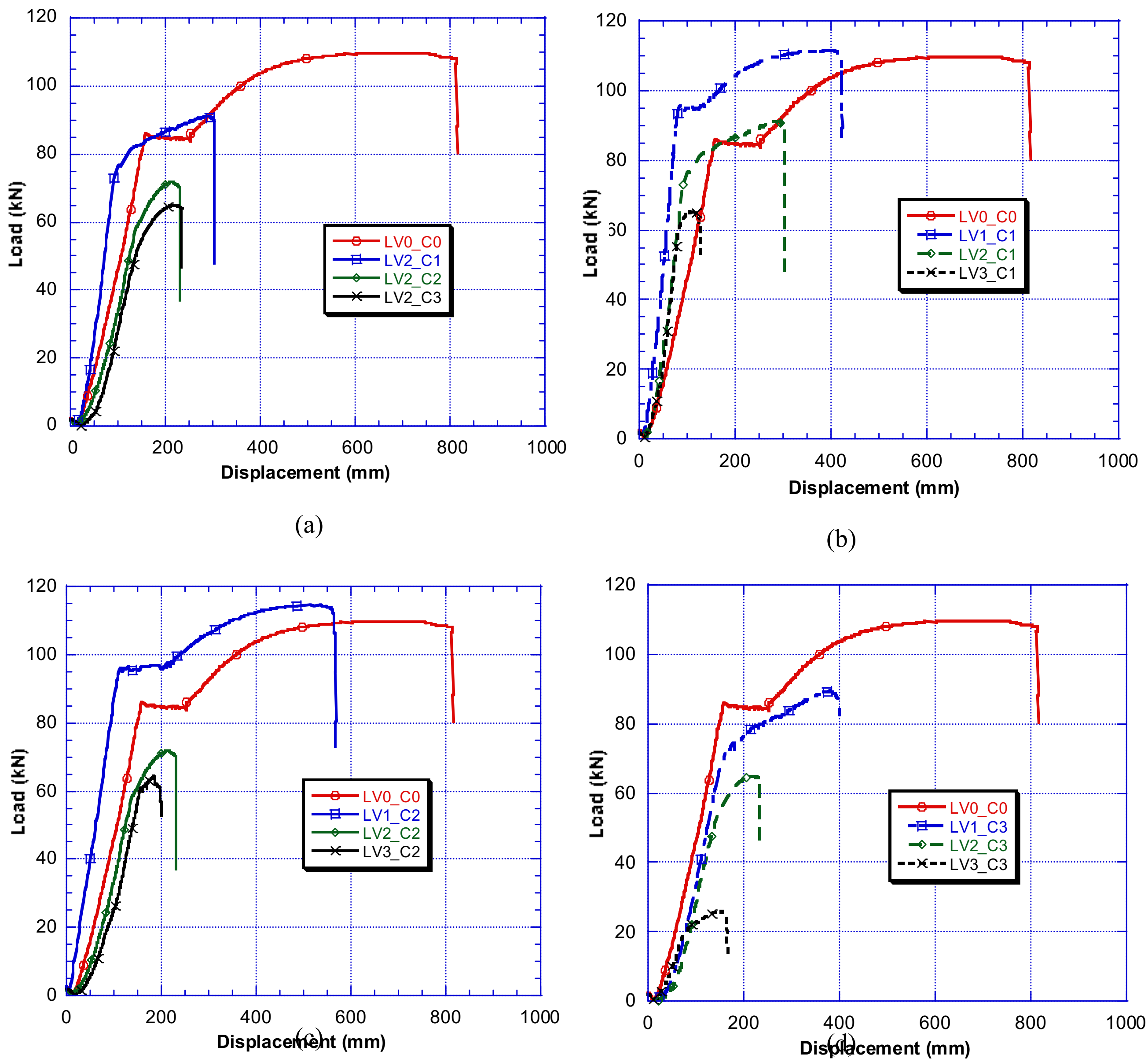


**Fig. 10** Load–displacement curves of reinforcing bars: **a** beam C0, C1, C2, C3; **b** beam C1; **c** beam C2; **d** beam C3

the bottom. Cracks from the bottom were spreading up to near the top in all beams C1, C2, C3. The beams were mainly damaged at the middle area, which significantly reduced the beam's bending capacity. Cracks are formed from the bottom of the beam up to the top of the beam. The higher the degree of corrosion, the shorter the crack length, which shows that the corroded rebars and the bond-stress slip between the rebar and the concrete are reduced, causing the concrete tensile zone to develop rapidly. Furthermore, the higher the degree of corrosion, the higher the distance between the cracks.

## 3 Numerical simulations

### 3.1 Input parameters

The numerical simulations were also conducted using ATENA, a commercial finite element software. The elements used to model the concrete is taken as a 3D Non-linear Cementitious 2, while reinforcing bars used steel bar elements. Bond-slip relationship were modeled for considering the bonding behavior of intact and corroded rebars and concrete. The bonding between reinforcements and concrete provides a vital role in mechanical behavior of corroded RC structures. The bond stress-slip relationship provided in CEB-FIP Model Code 1990 was adopted in the

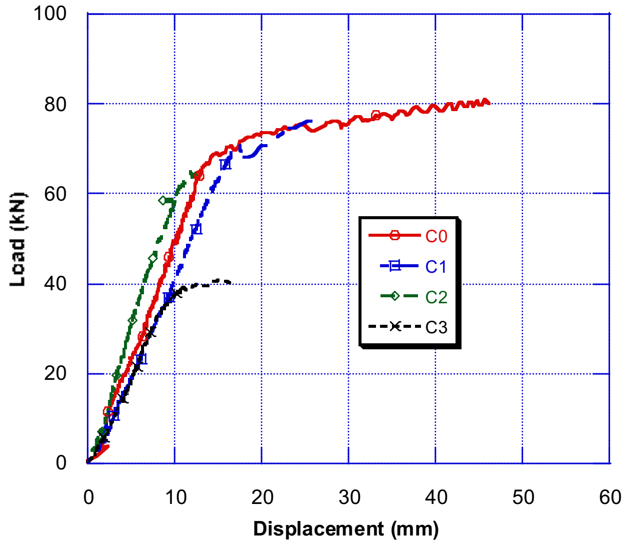


**Fig. 11** Load–displacement relationships of RC beams

numerical analysis. Three types of material have been defined by one elastic material for the steel plates at support and loading points, concrete material for the beam and reinforcement material.

#### 3.1.1 Concrete

In this study, the concrete element is described by 3D Nonlinear Cementitious 2 material model, default values of material parameters are generated based on the cube strength of concrete. The 3D Nonlinear Cementitious 2 material model is a nonlinear model that obeys the stress–strain law and Fixed crack model coefficient in Crack opening rule as shown in Fig. 13. In which, the required parameters of concrete that need to be declared include elastic modulus E, Poisson’s ratio $\mu$, tensile strength $f_t$, compressive strength $f_c$. Besides, the parameters of specific fracture energy $G_F$, fail, surface, excentricity, multiplier for

(a)

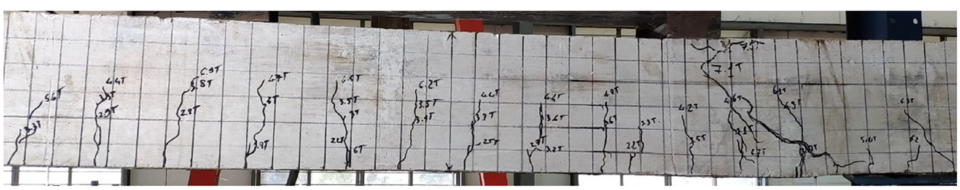

(b)

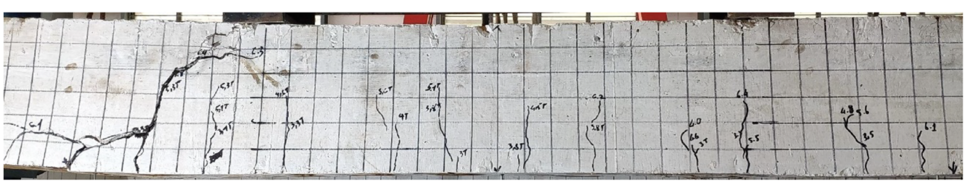

(c)

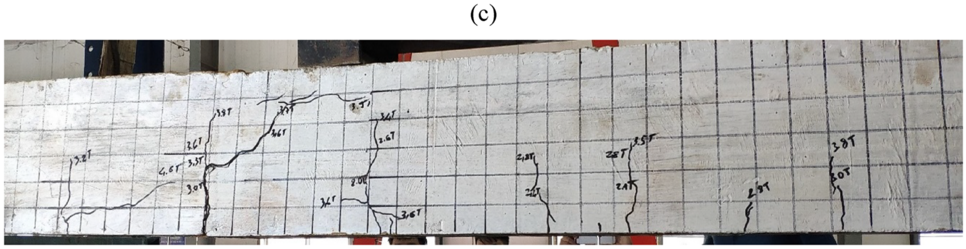

(d)

**Fig. 12** Crack patterns of RC beams: **a** beam C0; **b** beam C1; **c** beam C2; **d** beam C3

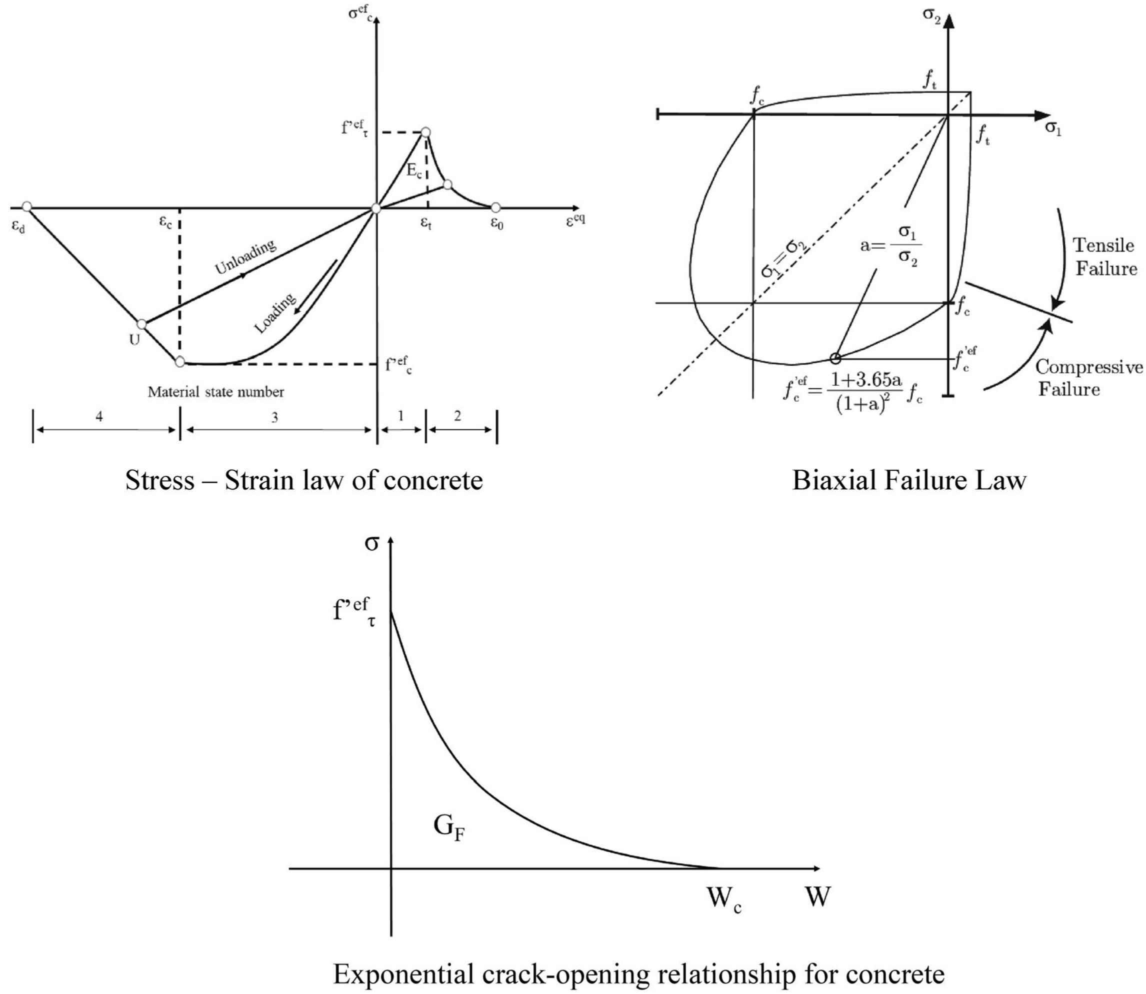


**Fig. 13.** 3D Nonlinear Cementitious 2 material model for concrete

the plastic flow dir β, specific material weight ρ, coefficient of thermal expansion α. At the same time, the compressive ductility of concrete is also assigned the values of critical compressive displacement $W_d$ and plastic strain at compressive strength $\varepsilon_{cp}$.

The data from Figs. 8, 11 and 12 show the effect of corrosion on the strength of concrete, beam displacement and crack development, respectively. The data from these figures and the analysis clearly show that corrosion severely degrades the behavior of concrete and reinforced concrete beams. Then, the characteristic values of each specimen under the effect of corrosion obtained from the experiment will be assigned to each corresponding FEM model, through changing the parameters in the 3D Nonlinear Cementitious 2 material model. When the parameters of the 3D Nonlinear Cementitious 2 material model are assigned directly from the experimental data, the FEM analysis results also accurately represent the effect of corrosion over time on the simulation models.

The mechanical properties of concrete used in the numerical model are provided in Table 5. Some parameters were taken from experiments, some were used from calculated values in TCVN 5574:2018 and remaining parameters were set as default values.

### 3.1.2 Reinforcements

In this study, reinforcing bars with 16 mm diameter were used for tension reinforcements and 10 mm diameter bars were for compression reinforcements. Meanwhile, the 6 mm diameter bars were employed for shear reinforcements. The mechanical properties of reinforcements are shown in Table 6.

For reinforcement element, it is described by 3D elastic isotropic model. 3D elastic isotropic model is a 3D linear model using the law of stress and deformation. To fit the model, bi-linear elastic perfectly plastic stress–strain was selected for analysis. In which, the required parameters of

**Table 5** Mechanical properties of concrete of un-corroded specimen

| Properties | Values | Remark |
|---|---|---|
| Elastic modulus (E) | 2.000E + 04 Mpa | TCVN: 5574:2018 |
| Poisson ratio (μ) | 0.2 | TCVN: 5574:2018 |
| Tensile strength ($f_t$) | 1.200E + 00 Mpa | TCVN: 5574:2018 |
| Compressive strength ($f_c$) | -1.660E + 01 Mpa | Experimental |
| Critical compressive displacement | 5E-04 m | ATENA |
| Plastic strain at compressive strength | -1.113E-03 | ATENA |
| Fail surface excentricity | 0.52 | ATENA |
| Multiplier for the plastic flow direction | 0 | ATENA |
| Specific material weight | 2.300E-02 MN/mE + 3 | TCVN: 5574:2018 |
| Coefficient of thermal expansion | 1.290E-01 1/K | ATENA |
| Fixed crack model coefficient | 1 | ATENA |

**Table 6** Degradation of mechanical properties of concrete

| RC beam | Compressive strength | Degradation of compressive strength (%) | Time, *t* (hr) |
|---|---|---|---|
| C1 | 504.7 | 16.6 | 720 |
| C2 | 399.8 | 17.2 | 1440 |
| C3 | 361.4 | 19.4 | 2160 |

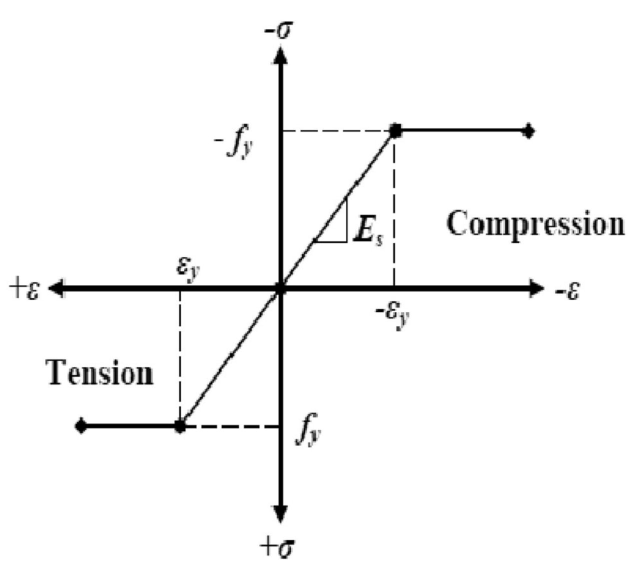


**Fig. 14** The bi-linear elastic-perfectly plastic stress–strain diagram for reinforcement

the reinforcement need to be declared, including Elastic modulus E and yield strength $\sigma_y$ as shown in Fig. 14.

The data from Figs. 9 and 10 show the effect of corrosion on the strength of reinforcement, beam displacement, respectively. The data from these figures and the analysis clearly show that corrosion severely degrades the behavior of reinforcement. Then, the characteristic values of each specimen under the effect of corrosion obtained from the experiment will be assigned to each corresponding FEM model, through changing the parameters in the 3D elastic isotropic model. When the parameters of the 3D elastic isotropic model are assigned directly from the experimental data, the FEM analysis results also accurately represent the effect of corrosion over time on the simulation models (Tables 7, 8).

As is known, the characteristics of a material will not change over time unless the material transforms into another material. Accordingly, the tensile stress of steel rebar is calculated according to the following formula 2.

$$\sigma = P/A, \tag{2}$$

where σ is tensile stress, P is tensile strength and A is cross section of steel bar.

Over time, under the influence of the environment, especially corrosion, the bearing capacity of steel structures seriously declines, but the characteristics of the material do not change, meaning the stress is constant. This is also completely suitable. When the bearing capacity decreases, the cross-sectional area will be changed by a corresponding density to ensure constant of stress.

In this study, due to experimental limitations, it was not possible to survey a large number of samples and cover all cases. But through experimental results, the decline in the

**Table 7** Mechanical properties of rebars

| Properties | | Values | Remark |
|---|---|---|---|
| Elastic modulus | | 200,000 MPa | TCVN: 5574:2018 |
| Uniaxial yield strength/ Uniaxial ultimate strength for steel | 16 mm diameter bar | 287/ 374 MPa | Experimental |
| | 12 mm diameter bar | 364/ 508 MPa | Experimental |
| | 6 mm diameter bar | 378/ 543 MPa | Experimental |
| Specific material weight | | 7.850E-02 MN/ mE + 3 | TCVN: 5574:2018 |
| Coefficient of thermal expansion | | 1.2E-05 1/K | ATENA |

**Table 8** Degradation of mechanical properties of steel bars and bending capacity

| RC beam | Tensile strength of steel bar | Degradation of tensile strength of steel bar (%) | Ultimate bending load (kN) | Time, *t* (hr) |
|---|---|---|---|---|
| C1 | 504.7 | 17.4 | 78.36 | 720 |
| C2 | 399.8 | 34.7 | 42.83 | 1440 |
| C3 | 361.4 | 41.0 | 28.94 | 2160 |

tensile strength of steel and compression of concrete over time can be completely predicted through the proposed regression method with two formulas 3 and 4, respectively.

$$R = -0.2342 + 0.1768 * t^{0.7145}, \quad (3)$$

$$R = 0.002 + 6.592 * t^{0.1376}. \quad (4)$$

Figure 15 shows the law of decreasing tensile capacity of steel and compression of concrete over time.

## 3.2 Constitutive material models

Finite element analysis for the reference beam CD, which were not subjected to corrosion and beams C1, C2, C3 to corrosion. Accurate simulation of the behavior of beams with corroded reinforcement is complicated due to the fact that corrosion varied along the longitudinal bars due to the presence of stirrups. Also, for a given beam, the average corrosion level differed for the tensile, compressive and transverse reinforcement. After the laboratory testing had been carried out the total weight loss of each bar was measured, so that the average loss of bar section could be calculated.

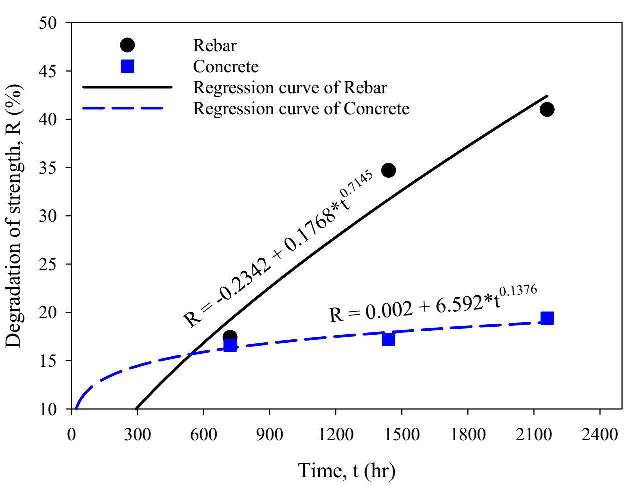


**Fig. 15** Degradation of tensile strength of steel bar and compressive strength of concrete versus time

In the analysis, the modeling of beam load and the shape can be done by finite element method using ATENA is shown in Fig. 16. This figure also shows the FE model of concrete beam and orientation of the longitudinal and transverse reinforcements. The isotropic multi axial elastic material model is used for steel elements in this study. The concrete and steel reinforcement interaction are modeled using "embedded region" constraint. Two steel plates are modeled at the load points to simulate the experimental setup and to avoid the local stress concentration. Tie constraint is used to model the interaction between steel plates and top surface of the concrete beam. The assembly of the RC beam is shown in Fig. 16. Meshing has been done after assembling concrete beam and steel reinforcement as shown in Fig. 16. A convergence study has been done to find the optimum mesh size. Mesh size in Fig. 16 of RC beam found to be appropriate for this study to maintain the uniform size for the whole beam.

## 3.3 Numerical results

In Fig. 17, comparison of load deflection behavior of beams found by experimentally and numerically is given. The load capacity of the control concrete beam (DC) obtained in the numerical analysis is consistent with the experimental one and the load deflection behavior of concrete beams (DC) are almost similar in both experimental and numerical results. In Fig. 17(b-d), the simulation is more complicated, the behavior is also very special, so the comparison results between experimental and the numerical results show that the stiffness of the beams is larger than experimentally. However, the numerical simulation results are quite good compared to that reported. This shows that numerical simulation from experimental results when there is sufficient input data is the basis for analyzing random and fuzzy problems to ensure the reliability of the problem when the variables are not clear.

# 4 Conclusions

The implementation of artificial corrosion in the conditions of this study through the periods of 720 h, 1440 h and 2160 h for 6 samples of reinforced concrete beams with reinforced diameters of 6 mm, 12 mm, and 16 mm, respectively. Assess the influence of corrosion over time on the behavioral characteristics of flexural beams such as bearing capacity, deflection, corrosion levels, growth, expansion, and propagation of traces. cracked. The obtained results add to the scientific knowledge of research on corrosion characteristics and can be applied to the design of steel structures under the effect of corrosion. Following conclusions are drawn.

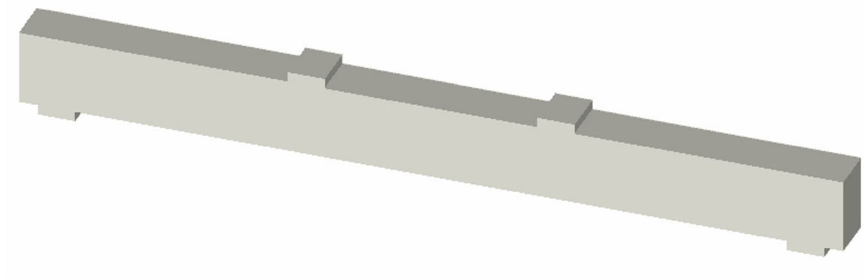

(a) FE modelling of concrete beam

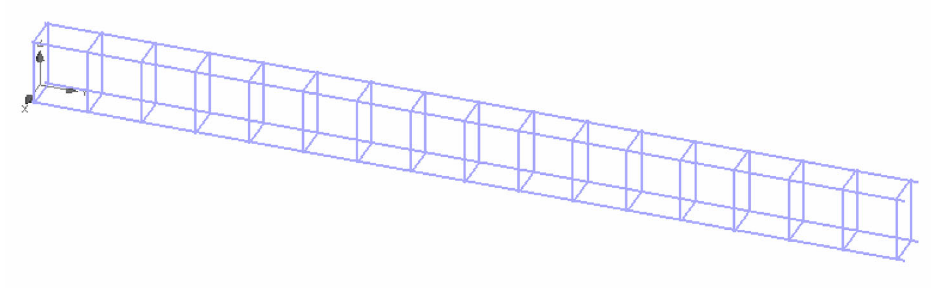

(b) FE modelling of reinforcement

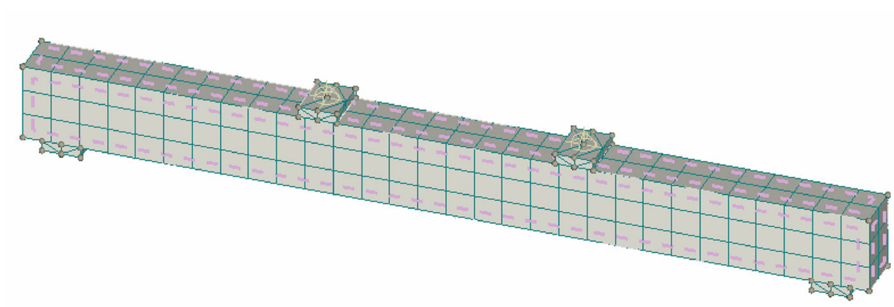

(c) Meshing of RC beam

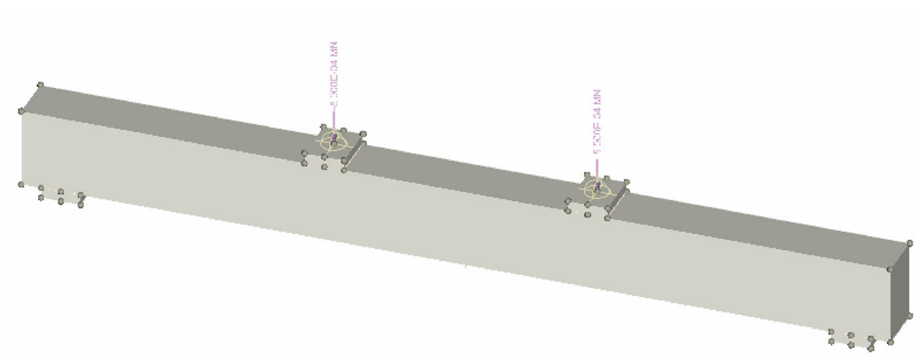

(d) Applied load and boundary condition

**Fig. 16** FE modeling of RC beams in ATENA

- Corrosion caused seriously effects on the behavior of reinforced concrete beams. Corrosion lead to reduction of the weight of rebar to lose 33.6% within 2160 h. Corrosion influenced to a rapid decrease in the bond-stress slip between rebar and concrete, while the rust surrounding the rebar increases the volume of reinforcement, causing concrete destruction from the inside. The diameter of the corroded rebar, the bond-stress slip

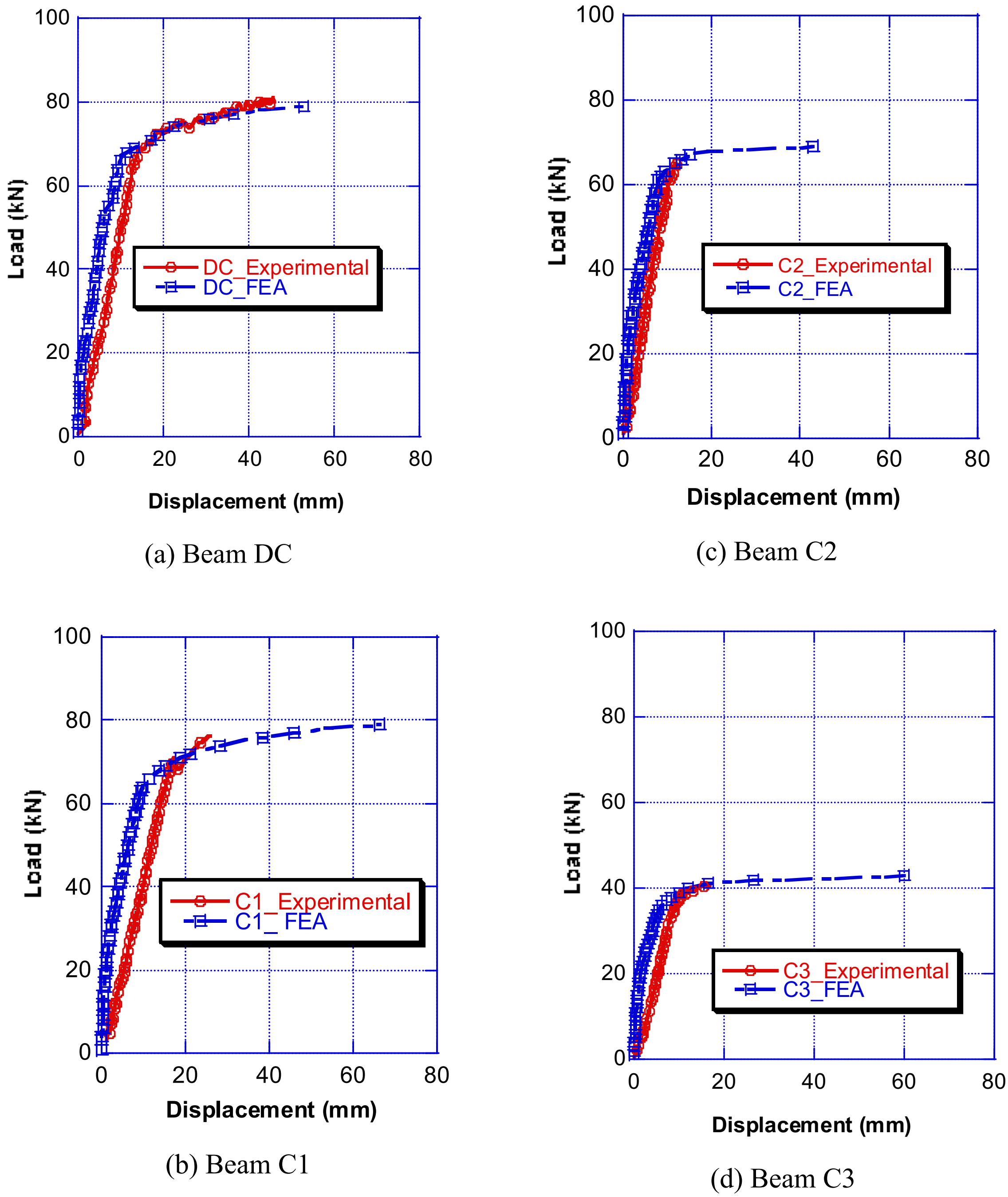


**Fig. 17** Load–deflection curves comparison for beams

between the rebar and the concrete, the rust surrounding the rebar directly is the bearing capacity of reduced up to 43.75% after 2160 h.

- Cracks are formed from the bottom of the beam up to the top of the beam. The higher the degree of corrosion, the shorter the crack length, which shows that the corroded rebars and the bond-stress slip between the rebar and the concrete are reduced, causing the concrete tensile zone to develop rapidly. Furthermore, the higher the degree of corrosion, the higher the distance between the cracks.
- Models and elements used in this study show a high compatibility in evaluating the bending behavior of beams as well as showing the characteristics of corrosion resistant steel working with concrete, especially describing the application of corrosion resistant steel. nonlinear treatment.

- Simulation is successful when the error of maximum force between experiment and simulation is less than 3%, error of displacement at maximum load between simulation and experiment is less than 1.8%. However, the behavior after reaching the maximum load value, the period of re-strengthening and destruction, the simulation method has not been implemented. This is also the limitation of the concrete element to the present time in the world.
- Simulation offers many advantages in determining the remaining workability of corroded steel structures when subjected to bending without doing any tests. In addition, predicting the dangerous cross-section of steel structures will support maintenance work to reduce risks for the project. The finite element method is important for predicting the cross-section of corroded steel components, including crack growth assessment.

**Acknowledgements** This work belongs to the project No. T2024- funded by Ho Chi Minh City University of Technology and Education, Vietnam.

## References

1. Bulletin (2011) Condition control and assessment of reinforced concrete structures exposed to corrosive environments (carbonation/chlorides). International Federation for Structural Concrete, Vol 59 of fib Bulletin, State-of-art report, 80 pages. https://www.fib-international.org/publications/fib-bulletins/condition-control-and-assessment-of-reinforced-concrete-struct-detail.html. (ISSN 1562–3610)
2. Chalhoub C, François R, Carcasses M (2020) Critical chloride threshold values as a function of cement type and steel surface condition. Cement and Concrete Research. 134:1–35. (https://doi.org/10.1016/j.cemconres.2020.106086). (ISSN: 0008–8846)
3. Li C, Jiang L, Li S (2020) Effect of limestone powder addition on threshold chloride concentration for steel corrosion in reinforced concrete. Cement and Concrete Research. 131
4. Ogunsanya IG, Hansson CM (2019) Detection of the critical chloride threshold of carbon steel rebar in synthetic concrete pore solutions. RILEM Technical Letters. 3:75–83. (https://doi.org/10.21809/rilemtechlett.2018.70. (ISSN 2518–0231)
5. Michel A, Pease BJ, Peterová A, Geiker MR, Stang H, Thybo AEA (2014) Penetration of corrosion products and corrosion-induced cracking in reinforced cementitious materials: Experimental investigations and numerical simulations. Cement and Concrete Composites. 47:75–86. (https://doi.org/10.1016/j.cemconcomp.2013.04.011). (ISSN: 0958–9465)
6. Torres-Acosta AA, Navarro-Gutierrez S, Terán-Guillén J (2007) Residual flexure capacity of corroded reinforced concrete beams. Engineering Structures. 29(6):1145–52. (https://doi.org/10.1016/j.engstruct.2006.07.018). (ISSN: 1873–7323)
7. Hariche L, Ballim Y, Bouhicha M, Kenai S (2012) Effects of reinforcement configuration and sustained load on the behaviour of reinforced concrete beams affected by reinforcing steel corrosion. Cement and Concrete Composites. 34(10):1202–1209. (https://doi.org/10.1016/j.cemconcomp.2012.07.010). (ISSN: 0958–9465)
8. Biswas RK, Iwanami M, Chijiwa N, Uno K (2020) Effect of non-uniform rebar corrosion on structural performance of RC structures: A numerical and experimental investigation. Construction and Building Materials. 230. (https://doi.org/10.1016/j.conbuildmat.2019.116908). (ISSN: 1879–0526)
9. Rodriguez J, Ortega LM, Casal J (1997) Load carrying capacity of concrete structures with corroded reinforcement. Construction and Building Materials. 11(4):239–248. (https://doi.org/10.1016/S0950-0618(97)00043-3). (ISSN: 1879–0526)
10. Ma Y, Guo Z, Wang L, Zhang J (2017) Experimental investigation of corrosion effect on bond behavior between reinforcing bar and concrete. Construction and Building Materials. 152:240–249. (https://doi.org/10.1016/j.conbuildmat.2017.06.169). (ISSN: 1879–0526)
11. Van Steen C, Verstrynge E, Wevers M, Vandewalle L (2019) Assessing the bond behaviour of corroded smooth and ribbed rebars with acoustic emission monitoring. Cement and Concrete Research. 120:176–86. (https://doi.org/10.1016/j.cemconres.2019.03.023). (ISSN: 0008–8846)
12. Yu L, François R, Dang VH, L'Hostis V, Gagné R (2015) Structural performance of RC beams damaged by natural corrosion under sustained loading in a chloride environment. Engineering Structures. 96:30–40. (https://doi.org/10.1016/j.engstruct.2015.04.001). (ISSN: 1873–7323)
13. Yamamoto T, Oyado M, Mikata Y, Kobayashi K, Shimomura T (2011) Systematic laboratory test on structural performance of corroded reinforced concrete and its utilization in practice. Modelling of Corroding Concrete Structures 5:113–124
14. Guo Z, Ma Y, Wang L, Zhang X, Zhang J, Hutchinson C, et al. (2020) Crack Propagation-Based Fatigue Life Prediction of Corroded RC Beams Considering Bond Degradation. Journal of Bridge Engineering. 25(8).
15. Ng PL, Gribniak V, Jakubovskis R, Rimkus A (2019) Tension stiffening approach for deformation assessment of flexural reinforced concrete members under compressive axial load. Structural Concrete. 20(6):2056–2068. (ISSN:1751–7648)
16. Santana Rangel C, Amario M, Pepe M, Yao Y, Mobasher B, Toledo Filho RD (2017) Tension stiffening approach for interface characterization in recycled aggregate concrete. Cement and Concrete Composites. 82:176–189. (https://doi.org/10.1016/j.cemconcomp.2017.06.009). (ISSN: 0958–9465)
17. Castel A, François R, Arliguie G (2000) Mechanical behaviour of corroded reinforced concrete beams—Part 1: Experimental study of corroded beams. Mater Struct 33(9):539–544
18. Castel A, François R, Arliguie G (2000) Mechanical behaviour of corroded reinforced concrete beams—Part 2: Bond and notch effects. Mater Struct 33(9):545–551
19. Imperatore S, Rinaldi Z, Spagnuolo S (2019) Influence of corrosion on the experimental behaviour of R.C. ties. Engineering Structures. 198. (https://doi.org/10.1016/j.engstruct.2019.109458). (ISSN: 1873–7323).
20. Kim, T. K. (2012). Study on cracking behavior of concrete due to rebar corrosion. Doctoral dissertation, Nagoya University, Japan.